frontiers in Earth Science

ORIGINAL RESEARCH
published: 04 August 2021
doi: 10.3389/feart.2021.707869

Structural Inheritance Controls Strain Distribution During Early Continental Rifting, Rukwa Rift

Folarin Kolawole[1,2], Thomas B. Phillips[3], Estella A. Atekwana[4] and Christopher A.-L. Jackson[5]*

[1]School of Geosciences, University of Oklahoma, Norman, OK, United States, [2]BP America, Houston, TX, United States, [3]Science Labs, Department of Earth Sciences, Durham University, Durham, United Kingdom, [4]Department of Earth Science, University of Delaware, Newark, DE, United States, [5]Department of Earth and Environmental Sciences, The University of Manchester, Manchester, United Kingdom

Little is known about rift kinematics and strain distribution during the earliest phase of extension due to the deep burial of the pre-rift and earliest rift structures beneath younger, rift-related deposits. Yet, this exact phase of basin development ultimately sets the stage for the location of continental plate divergence and breakup. Here, we investigate the structure and strain distribution in the multiphase Late Paleozoic-Cenozoic magma-poor Rukwa Rift, East Africa during the earliest phase of extension. We utilize aeromagnetic data that image the Precambrian Chisi Shear Zone (CSZ) and bounding terranes, and interpretations of 2-D seismic reflection data to show that, during the earliest rift phase (Permo-Triassic 'Karoo'): 1) the rift was defined by the Lupa border fault, which exploited colinear basement terrane boundaries, and a prominent intra-basinal fault cluster (329° ± 9.6) that trends parallel to and whose location was controlled by the CSZ (326°); 2) extensional strain in the NW section of the rift was accommodated by both the intra-basinal fault cluster and the border fault, where the intra-basinal faulting account for up to 64% of extension; in the SE where the CSZ is absent, strain is primarily focused on the Lupa Fault. Here, the early-rift strain is thus, not accommodated only by the border fault as suggested by existing magma-poor early-rift models; instead, strain focuses relatively quickly on a large border fault and intra-basinal fault clusters that follow pre-existing intra-basement structures; 3) two styles of early-rift strain localization are evident, in which strain is localized onto a narrow discrete zone of basement weakness in the form of a large rift fault (Style-1 localization), and onto a broader discrete zone of basement weakness in the form of a fault cluster (Style-2 localization). We argue that the CSZ and adjacent terrane boundaries represent zones of mechanical weakness that controlled the first-order strain distribution and rift development during the earliest phase of extension. The established early-rift structure, modulated by structural inheritance, then persisted through the subsequent rift phases. The results of our study, in a juvenile and relatively well-exposed and data-rich rift, are applicable to understanding the structural evolution of deeper, buried ancient rifts.

Keywords: continental rifting, tectonic strain, normal faults, rukwa rift basin, east african rift system

OPEN ACCESS

Edited by:
James D Muirhead,
The University of Auckland,
New Zealand

Reviewed by:
Giacomo Corti,
National Research Council (CNR), Italy
Damien Delvaux,
Royal Museum for Central Africa,
Belgium

****Correspondence:***
Folarin Kolawole
folarin.kol@gmail.com

Specialty section:
This article was submitted to Structural Geology and Tectonics, a section of the journal Frontiers in Earth Science

Received: *10 May 2021*
Accepted: *22 July 2021*
Published: *04 August 2021*

Citation:
Kolawole F, Phillips TB, Atekwana EA and Jackson CA-L (2021) Structural Inheritance Controls Strain Distribution During Early Continental Rifting, Rukwa Rift. Front. Earth Sci. 9:707869. doi: 10.3389/feart.2021.707869

INTRODUCTION

Tectonic extension of the continental lithosphere is typically accommodated by the brittle deformation of the upper crust, demonstrated by the emergence of normal fault populations (Cowie et al., 2005; Agostini et al., 2011; Muirhead et al., 2016, 2019). Some classic models for the evolution of continental rifts, suggest that during the early phase of extension, strain is initially accommodated by the development of distributed normal faults, with strain subsequently localizing onto a few large faults and subsequently migrating to the rift axis (e.g., Chorowicz, 2005; Gawthorpe and Leeder, 2008; Nixon et al., 2016; Naliboff et al., 2017). However, a comparison of juvenile, magma-rich and magma-poor segments of narrow rifting along the East African Rift System (EARS) show that in contrast to the magma-rich rift basins where strain is accommodated by both the large basin-bounding faults (border faults) and intra-basinal structures, the border faults accommodate most (~90%) of the strain in the magma-poor rift segment (Muirhead et al., 2019). Elsewhere along the EARS, the incipient (<3 Ma) magma-poor Zomba Graben, southern Malawi Rift, has already witnessed the localization of strain in the rift axis, with the related faults presently accounting for up to 55% (±24) of the extensional strain (Wedmore et al., 2020a). The evidence presented in these studies indicate that early-phase extensional strain along magma-poor continental rifts may or may not be primarily accommodated by only the border faults. Thus, there is a need to better understand other mechanisms that can facilitate early focusing of intra-basinal faulting and extensional strain in magma-poor continental rifts.

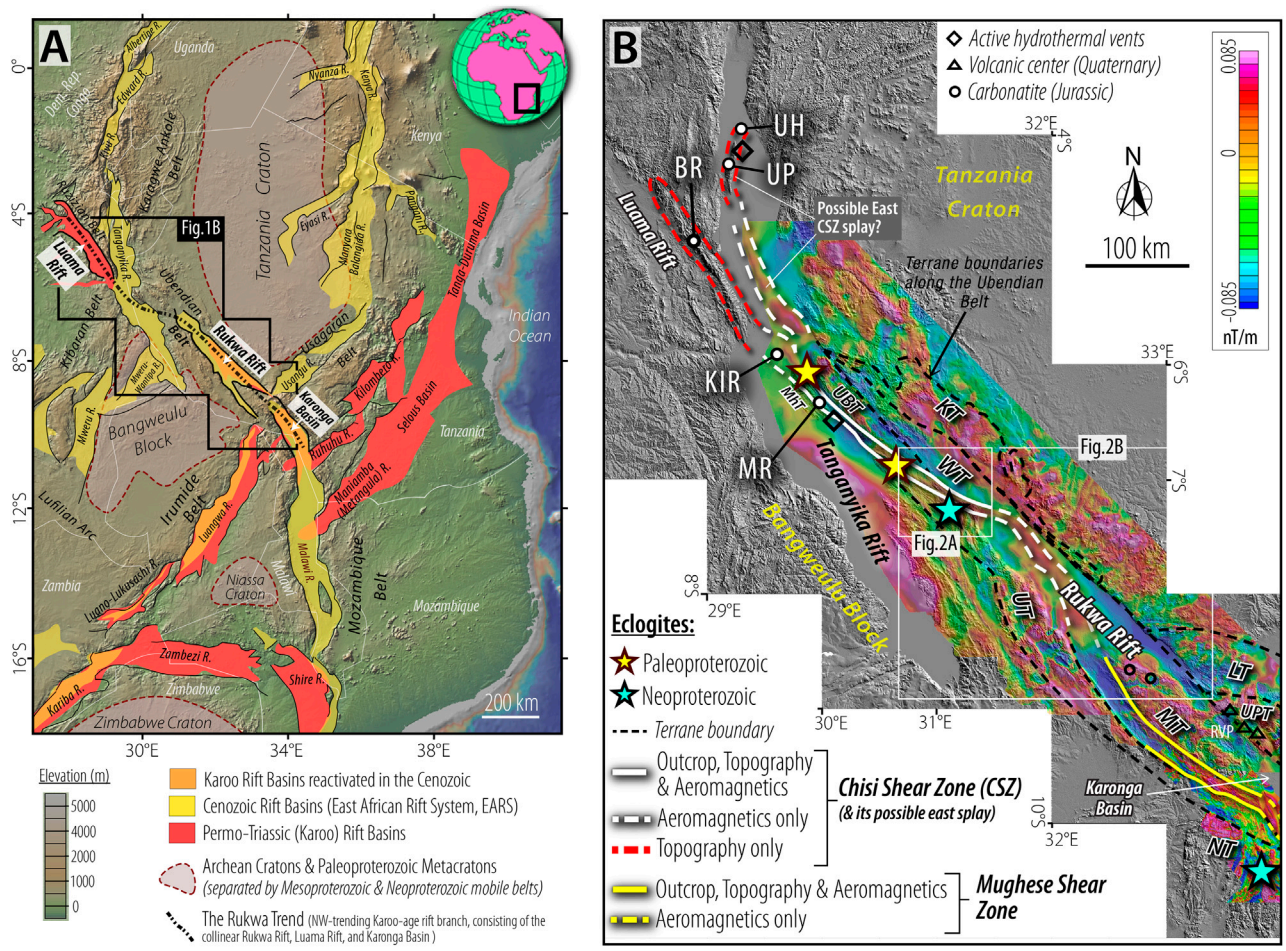

FIGURE 1 | (A): Map of East Africa showing the Permo-Triassic (i.e., Karoo rift system) rift segments, and the currently active rift segments (i.e., East African Rift System). **(B)**: Shuttle Radar Topography Mission (SRTM) Digital Elevation Model (DEM) hillshade map covering the Rukwa Rift Trend, overlaid with the vertical derivative aeromagnetic of SW Tanzania. Black dashed lines represent boundaries of the Precambrian terranes of the Rukwa Rift Trend (after Daly, 1988; Lenoir et al., 1994; Delvaux et al., 2012; Lemna et al., 2019; Heilman et al., 2019). Locations of Proterozoic eclogites in the Ubendian Belt are from Boniface et al. (2012) and Boniface and Schenk (2012). Locations of hydrothermal vents and Mesozoic-Cenozoic igneous centers (volcanics and carbonatites) are obtained from Hodgson et al. (2017). See uninterpreted aeromagnetic and hillshade maps in **Supplementary Figures 1**, **2**. Geomorphic features: BR (Busindi Ridge), KIR (Kavala Island Ridge), MR (Mahale Ridge), UP (Ubwari Peninsula), UH (Ubwari Horst). Terranes of the Ubendian Belt: KT (Katuma Terrane), LT (Lupa Terrane), MT (Mbozi Terrane), MhT (Mahale Terrane), RVP (Rungwe Volcanic Province), UBT (Ubende Terrane), UPT (Upangwa Terrane), UT (Ufipa Terrane), WT (Wakole Terrane).

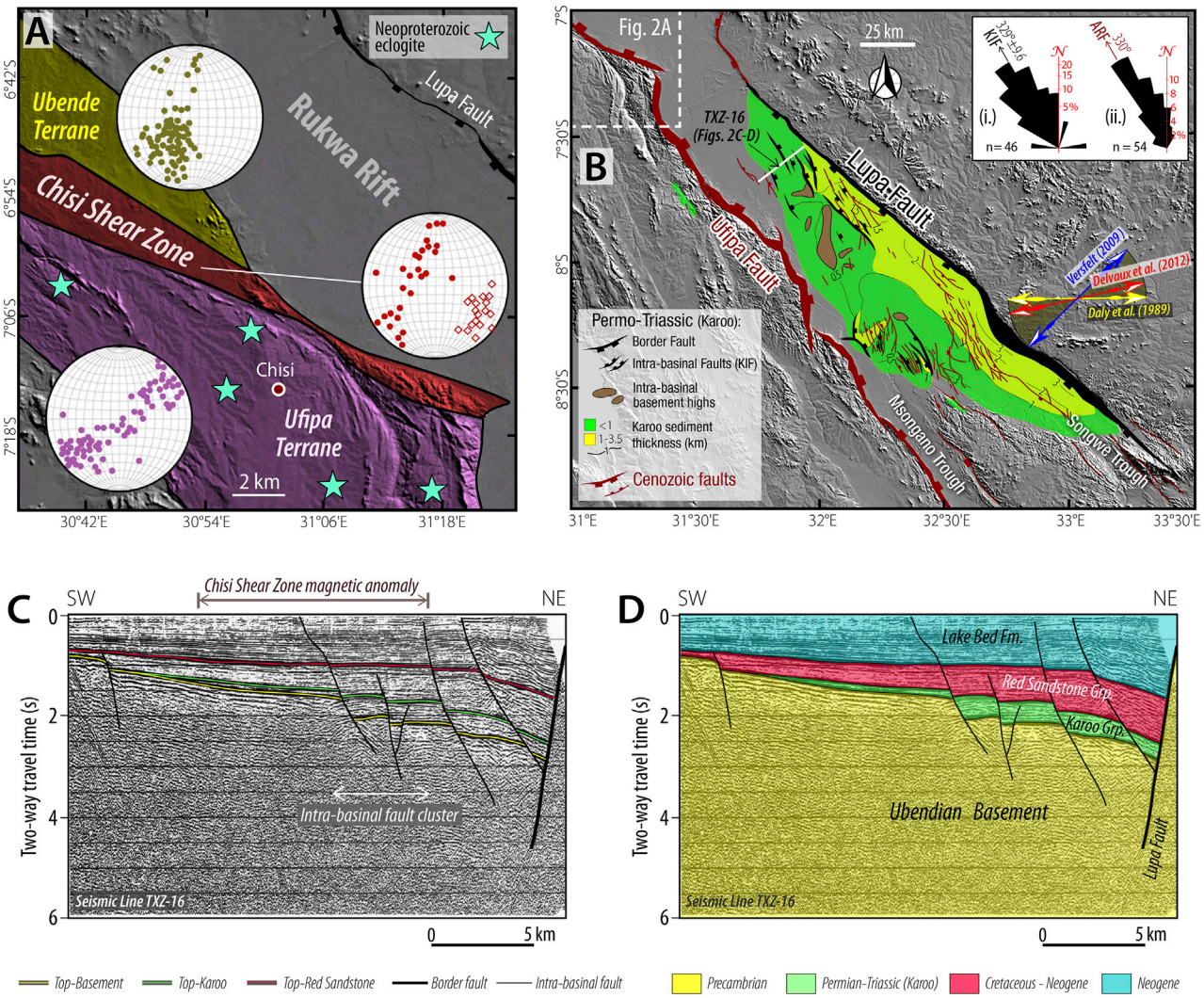

FIGURE 2 | (A): Shuttle radar digital elevation model (DEM) hillshade map of the NW Rukwa Rift shoulder (see **Figure 1B**, **2B** for location) showing the Precambrian Chisi Shear Zone exposure and its bounding basement terranes. The plots of equal area stereographic projection (lower hemisphere) show the poles to planes of gneissic foliation (filled circles), and poles of mineral elongation lineation and some fold axes of asymmetric intrafolial folds (diamonds in the Chisi Shear Zone stereonet) measured in field outcrops (from Boven et al., 1999). These structures represent the metamorphic basement fabrics of the basement. Locations of Neoproterozoic eclogites in the Chisi area are from Boniface and Schenk (2012). **(B)**: Map of the Rukwa Rift showing the interpreted Karoo and post-Karoo structural elements (structural elements are from Morley et al., 1992, 1999). Arrows represent the previously published inferred Karoo extension directions. *Inset:* Frequency-azimuth distribution plot for ***(i.)*** Karoo-age (Permo-Triassic) intra-basinal faults (KIF) with black arrow indicating their mean trend and standard error (measured in this study), and ***(ii.)*** All (Permian to Quaternary) Rukwa Rift faults (ARF) with their mean trend shown as brown arrow (digitized from Morley et al., 1992). **(C–D)**: 2-D seismic reflection profile line TXZ-16 and interpretation (modified from Morley et al., 1999; see location in **Figure 2B**) showing the major stratigraphic boundary horizons, the Lupa border fault, and intra-basinal faults.

Since continental rifts typically develop in previously deformed lithosphere (Wilson, 1966; Dewey and Spall, 1975; Buiter and Torsvik, 2014), the distribution of early-phase strain in magma-poor rifts can be complex due to the interaction between faults that exploit or reactivate pre-existing structures, and those that form independently of any pre-existing structure (e.g., Manatschal et al., 2015; Kolawole et al., 2018; Ragon et al., 2019; Schiffer et al., 2019; Phillips et al., 2019a,b; Heilman et al., 2019; Osagiede et al., 2020; Wang et al., 2021). Overall, very little is known about the earliest phase of continental extension, and even less of how strain is partitioned along inherited structures; this reflects the fact that the associated structures and related stratigraphic record are typically deeply buried beneath younger (i.e., post-rift or later rift phase) sequences and are thus difficult to image with geophysical data, or are overprinted by later tectonic events (e.g., post-rift plate collision). This knowledge gap limits a fuller understanding of the spectrum of processes that govern continental rifting and breakup in space and time.

The EARS (**Figure 1A**) is the largest active continental rift system on Earth. This system, which formed by the stretching of

previously deformed lithosphere, is characterized by segments that span the major stages of continental rifting from inception to transitional crust (e.g., Daly et al., 1989; Hayward and Ebinger, 1996; Delvaux, 2001; Chorowicz, 2005; Ebinger, 2005). We integrate available geophysical and geological datasets from the multiphase magma-poor Rukwa Rift (**Figures 1A,B**, **2A–D**) to explore how strain was distributed during the earliest phase of extension, and investigate the dominant controls. We show that the potentially lithosphere-scale Precambrian Chisi Shear Zone (CSZ) and its adjacent terrane boundaries (**Figure 1B**; Lemna et al., 2019; Heilman et al., 2019) represent major zones of pre-rift basement mechanical weakness that controlled the location, structure, and evolution of both the border and intra-basinal faults during the earliest phase of continental extension. We show how the geometry of the CSZ controlled along-rift variations in the early-phase tectonic extension and overall basin geometry, the effects of which persist through and thus influence the later rift geometry. We also expand our analysis to the nearby Luama Rift (located in DRC), which is coeval, colinear with, and parallel to the Rukwa Rift; both basins representing structural elements along a NW-trending Karoo-age rift branch herein referred to as "the Rukwa Trend" (**Figure 1A**). Our results resolve a long-standing controversy related to the geometrical structure and kinematics of rifting in this part of the East African Rift System.

GEOLOGICAL SETTING

The Precambrian (Pre-Rift) Basement of the Rukwa Trend

The crystalline basement of the Rukwa Trend is composed of the metamorphic and igneous rocks of the Precambrian (1.95–1.85 Ga) Ubendian Belt, which formed during the collision of the Archean Tanzania Craton and the Bangweulu Block, and which comprises the Ufipa, Katuma, Wakole, Lupa, Mbozi, Ubende, and Upangwa terranes (**Figures 1A,B**; Daly, 1988; Lenoir et al., 1994). This orogenic belt, which is defined by several NW-trending terranes (2.1–2.025 Ga) that are bounded by steeply dipping, ductile, amphibolite facies, strike-slip shear zones (**Figure 1B**; Daly, 1988; Lenoir et al., 1994; Theunissen et al., 1996; Kolawole et al., 2018). The terranes are composed of amphibolite to granulite facies gneisses with foliations that dominantly trend NW-SE and commonly steepen near the terrane boundaries (Lenoir et al., 1994). Although relative rare compared to gneisses, other metasediments along the belt consists of mica schists, marbles, meta-anorthosites, and ferruginous quartzites (Lenoir et al., 1994).

The geochronology, geochemistry, and metamorphic structure of the Ubendian Belt suggests that it formed in response to multiple episodes of wrench tectonic events (Theunissen et al., 1996) with phases of subduction extending from the Paleoproterozoic to the Neoproterozoic (Ganbat et al., 2021). The orogenic belt first developed during a phase of collisional orogeny along the SW margin of the Tanzanian Craton (ca 2.1–2.0 Ga), after which the belt experienced two episodes of wrench tectonics consisting of an initial phase of dextral strike-slip shear at ca. 1.8–2.0 Ga, followed by a ductile-brittle sinistral strike-slip reactivation in the Neoproterozoic (Lenoir et al., 1994). This Neoproterozoic shear reactivation recorded the development of thick mylonite and blastomylonite zones with low-grade metamorphic assemblages along shear zones that bound the terranes. The terranes and associated fabrics which are observable in basement exposures along the flanks of the Phanerozoic Rukwa Rift, are suggested to have exerted some control on the development of the basin (Wheeler and Karson, 1994; Theunissen et al., 1996; Klerkx et al., 1998; Boven et al., 1999; Heilman et al., 2019; Lemna et al., 2019).

The Chisi Shear Zone

Along the Ubendian Belt, the Chisi Shear Zone (CSZ) is a prominent shear zone which separates the Ufipa Terrane to the southwest, from the Wakole and Ubende Terranes to the northeast (**Figure 1B**). The structure was initially identified as the "Ikulu series" or "Ikulu Terrane", a broad (6–12 km-wide in Chisi area) shear belt composed of amphibolite, micaschist, and meta-calcareous rocks with high pressure blueschist or eclogitic associations (Lenoir et al., 1994; Boven et al., 1999). The mafic high-pressure sequences along the shear zone were interpreted to represent disrupted remnants of deeply subducted ophiolites (Smirnov et al., 1973; Lenoir et al., 1994; Klerkx et al., 1998; Sklyarov et al., 1998).

Along the "Ikulu" structure, amphibolites and amphibole gneisses exhibit metamorphic foliation with planes that dominantly strike WNW-ESE and dip steeply to the NNE and S-SSW (stereographic plot with red filled circles in **Figure 2A**; Theunissen et al., 1996; Boven et al., 1999). The rocks also exhibit mineral elongation lineation and some fold axes of asymmetric intrafolial folds that generally trend NW-SE and plunge shallowly-to-moderately to the ESE-SE (stereographic plot with open diamonds in **Figure 2A**). Mylonitic rocks along the SW margin of the granulitic Ubende Terrane exhibit P-T characteristics and shear fabrics suggesting an uplift and exhumation of the terrane relative to the felsic Ufipa Terrane on the SW flank of the "Ikulu" structure (Theunissen et al., 1996; Sklyarov et al., 1998; Boven et al., 1999). More detailed petrographic and geochemical investigation of the eclogites reveal striking similarities with oceanic island-arc volcanic rocks (Boniface and Schenk, 2012). Geochronologic analyses indicate a clustering of Paleoproterozoic eclogites to the northern segment of the structure (near Lake Tanganyika) and Neoproterozoic eclogites to the south (e.g., Chisi area and northern Malawi) (**Figure 1B**), suggesting multiple cycles of subduction-related orogenic events along the structure (Boniface et al., 2012; Boniface and Schenk, 2012; Ganbat et al., 2021). Thus, the "Ikulu" domain was proposed to be the primary Late Proterozoic (Pan African Orogeny) suture zone between the Tanzania and Bangweulu Cratons along the Ubendian Belt (Boniface and Schenk, 2012).

Further, the magnetic-high anomaly expression of the "Ikulu" domain, created by the dominance of mafic rocks along the belt, defines a prominent regional magnetic lineament that extends southeast beneath the Rukwa Rift sedimentary cover, sub-parallel to the northwest trend of the rift (**Figure 1B**; Lemna et al., 2019;

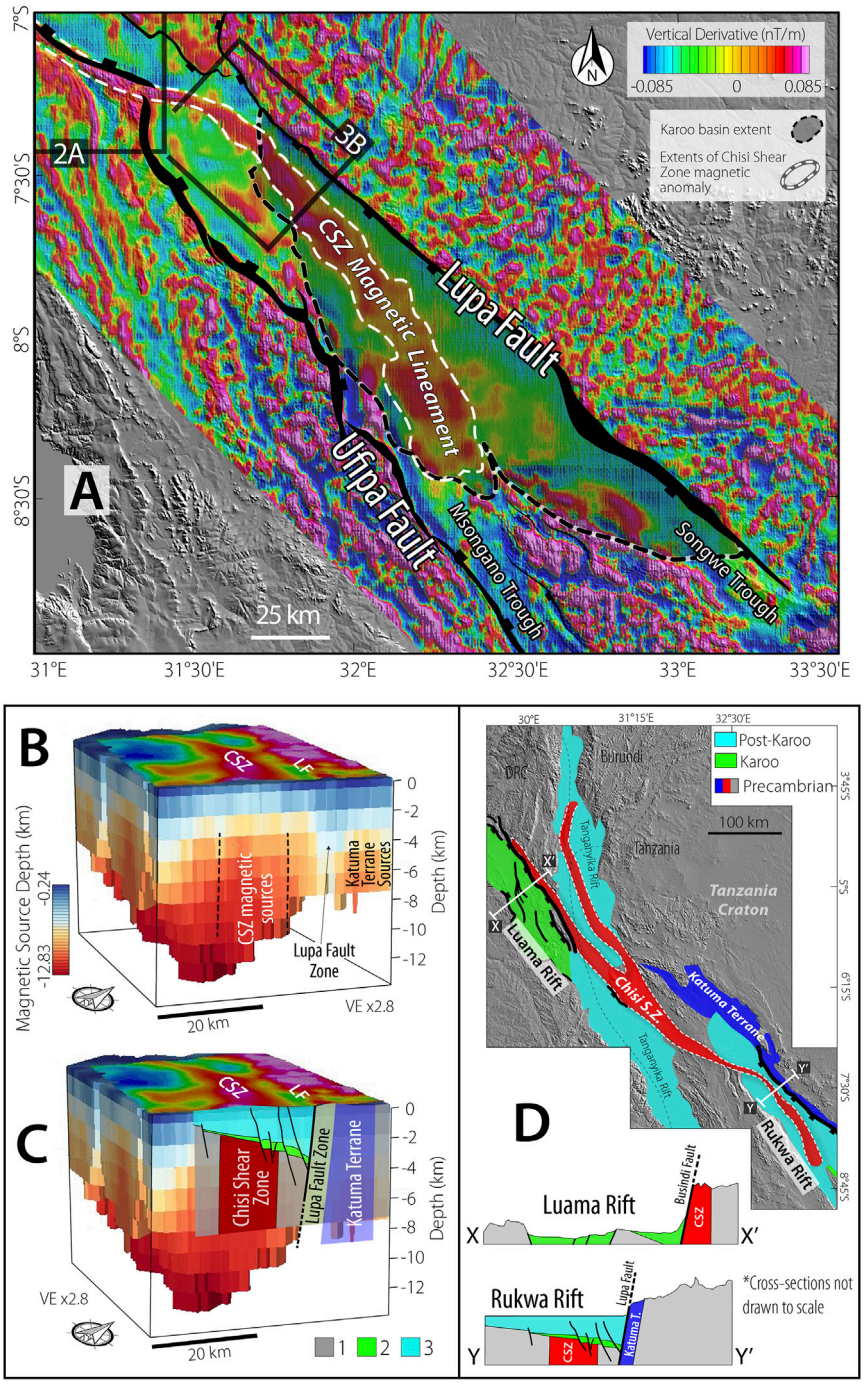

FIGURE 3 | (A): Vertical derivative of the aeromagnetic grid overlaid on satellite Digital Elevation Model (DEM) hillshade map, showing the rift border faults, rift shoulder basement fabrics and the aeromagnetic signature of the Chisi Shear Zone (CSZ) along the rift axis. See uninterpreted aeromagnetic maps in **Supplementary Figure 1**. **(B)**: 3-D gridded block of the Source Parameter Imaging (SPI) solutions from the transform of the aeromagnetic grid, showing the subsurface extents and geometry of CSZ and the shallower Katuma Terrane magnetic sources. **(C)**: 3-D gridded block overlaid with interpretations of the rift faults and simplified stratigraphy (interpretations from 2-D seismic line TXZ-16 of Morley et al., 1999 shown in **Figure 2C**). Stratigraphic units shown: 1 = Precambrian basement), 2 = Permo-Triassic (Karoo Grp.) sequences, 3 = Post-Karoo sequences i.e., Red Bed Grp. and Lake Bed Fm.). **(D):** Regional satellite DEM hillshade map showing the >600 km extent of the CSZ and its relationships with the Rukwa and Luama segments of the Rukwa Trend. The Luama Rift cross-section is based on legacy geologic maps and satellite DEM, and that of the Rukwa Rift is based on 2-D seismic data interpretation, satellite DEM, and aeromagnetics.

Heilman et al., 2019). Since the Chisi area of Tanzania represents a type-locality for the detailed studies of the structural fabrics, geochemistry, and petrology of the structure (Theunissen et al., 1996; Boven et al., 1999; Boniface and Schenk, 2012), the structure was recently officially re-introduced as "Chisi Shear Zone" (Lemna et al., 2019) or "Chisi Suture Zone" (Heilman et al., 2019). However, in this current study, we adopt the name "Chisi Shear Zone" to refer to the structure.

Phanerozoic Rifting Along the Rukwa Trend

The present-day configuration of the Rukwa Trend consists of multiple colinear, NNW-trending rift basins (Rukwa, Karonga, and Luama basins) that initially developed during Permo-Triassic (Karoo) phase of rifting (e.g., Delvaux, 2001). All three basins were reactivated by extensional tectonics in the Cretaceous (Roberts et al., 2010, 2012). However, only the Rukwa Rift and Karonga Basin (**Figure 1A**) experienced significant reactivation in the Cenozoic, and they are still currently active (e.g., Morley et al., 1999; Delvaux, 2001; Chorowicz, 2005). The Rukwa Rift, the primary focus of this study, currently defines a graben and is bounded to the northeast by the Lupa Fault and to the southwest by the Ufipa Fault (**Figure 2B**; Heilman et al., 2019; Morley et al., 1999). The basin initially developed as a NE-dipping half graben (with a shallow graben geometry only in the NW) during the Karoo rifting phase, bounded to the northeast by the principal border fault, the Lupa Fault (**Figures 2C,D**). The Karoo intra-basinal faults (KIF) and basement highs predominantly trend NNW, oblique to the Lupa Fault strike (**Figure 2B**). Estimates of the Karoo-age extension direction vary from NE-SW to E-W (**Figure 2B**).

DATASET AND METHODOLOGY

Along the Rukwa Trend, we compile structural mapping and structural measurement data from published 2-D seismic data (e.g., **Figure 2C**; Morley et al., 1999) and integrate these with aeromagnetic data (**Supplementary Figures S1A–B**) and Shuttle radar digital elevation model (DEM) (**Supplementary Figures S2A–B**).

Aeromagnetic Data, Shuttle Radar Topographic Data, and their Analyses

We use aeromagnetic data to map key pre-rift intra-basement structures along the axis of the Rukwa Rift and along-trend of the rift. We applied derivative filters to the aeromagnetic grid to enhance structural features (**Figure 3A**), and mathematical transforms to estimate the depths to magnetic sources in the basement (**Figures 3B–D**; see **Supplementary Material** information).

The aeromagnetic data (**Supplementary Figure S1A**), collected between 1977–1980 with flight height of 200 m and a flight line spacing of 1 km, was provided by the South African Council for Geoscience. First, we reduced the data to the magnetic pole (RTP) to correct for latitude-dependent skewness (Baranov, 1957), after which we applied a vertical derivative filter to better resolve magnetic gradients associated with structural features (**Figure 3A**, **Supplementary Figure S1B**) (Salem et al., 2007; Kolawole et al., 2017, 2018; Heilman et al., 2019). In this study, we delineate the boundaries of the Chisi Shear Zone along the edges of the high magnetic anomaly lineament in the vertical derivative map of the aeromagnetic grid. In areas where aeromagnetic data is not available, we augmented the basement mapping with 30 m-resolution Shuttle Radar Topography Mission (SRTM) Digital Elevation Model (DEM) hill shade maps (**Supplementary Figures S2A–B**).

Structural Data From Seismic Interpretation

We establish the initial (i.e., Karoo rift phase) geometry of the Rukwa Rift and related faults using published seismic reflection profiles, and associated fault trace maps and sediment thickness maps ("Karoo Isopach") presented by Morley et al. (1992, 1999). We also calculate along-rift variations in Karoo-age tectonic extension (geometrically-restored to Karoo time surface; **Figures 4A–D**) accommodated by slip on the Lupa Fault and intra-basinal faults, again using data published by Morley et al. (1992). We integrate these structural data with aeromagnetic data analysis to investigate the influence of the pre-rift basement structure on the early-rift structure and evolution of the Rukwa Rift (**Figures 4A–C**).

RESULTS

3-D Geometry and Extent of the CSZ

The petrology and geochemistry, local structure, and topographic expression of the CSZ is well-constrained in the Chisi area, located on the NW flank of the Rukwa Rift (**Figures 1B**, **2A**; Theunissen et al., 1996 and Boven et al., 1999; Boniface and Schenk, 2012). Field observations show that the CSZ is dominated by steep, NE- and SW-dipping, metamorphic fabrics hosted by eclogite facies rocks (**Figure 2A**). At this location, the CSZ is characterized by a prominent NW-trending, positive magnetic anomaly lineament (**Figure 1B**) and a topographic ridge (**Figure 2A** and **Supplementary Figure S2A**). Based on its distinct geophysical and geomorphic expression, as well as known field locations of eclogite rocks, we map the northwestward and southeastward continuations of the CSZ system beneath the Rukwa Rift and along the northeastern boundary zone of the Luama Rift respectively (**Figure 1B**).

Northwest of the Chisi area, the CSZ associated structures are colinear with the subaerial Mahale Ridge and the submerged Kavala Island Ridge (submerged beneath Lake Tanganyika), and continues northwest into the Busindi Ridge which itself represents the footwall of the Busindi border fault of the Luama Rift (**Figure 1B**, **Supplementary Figure S2A**). Along the Luama Rift, the inferred CSZ extension represents the boundary between the Kibaran Belt (to the south) and the Ruzizian Belt to the north (**Figure 1A**). Based on the occurrence of a prominent high magnetic lineament extending NNW across Lake Tanganyika from the northernmost known CSZ-related eclogite exposure, a possible East CSZ splay is delineated to continue northward and link with the N-trending

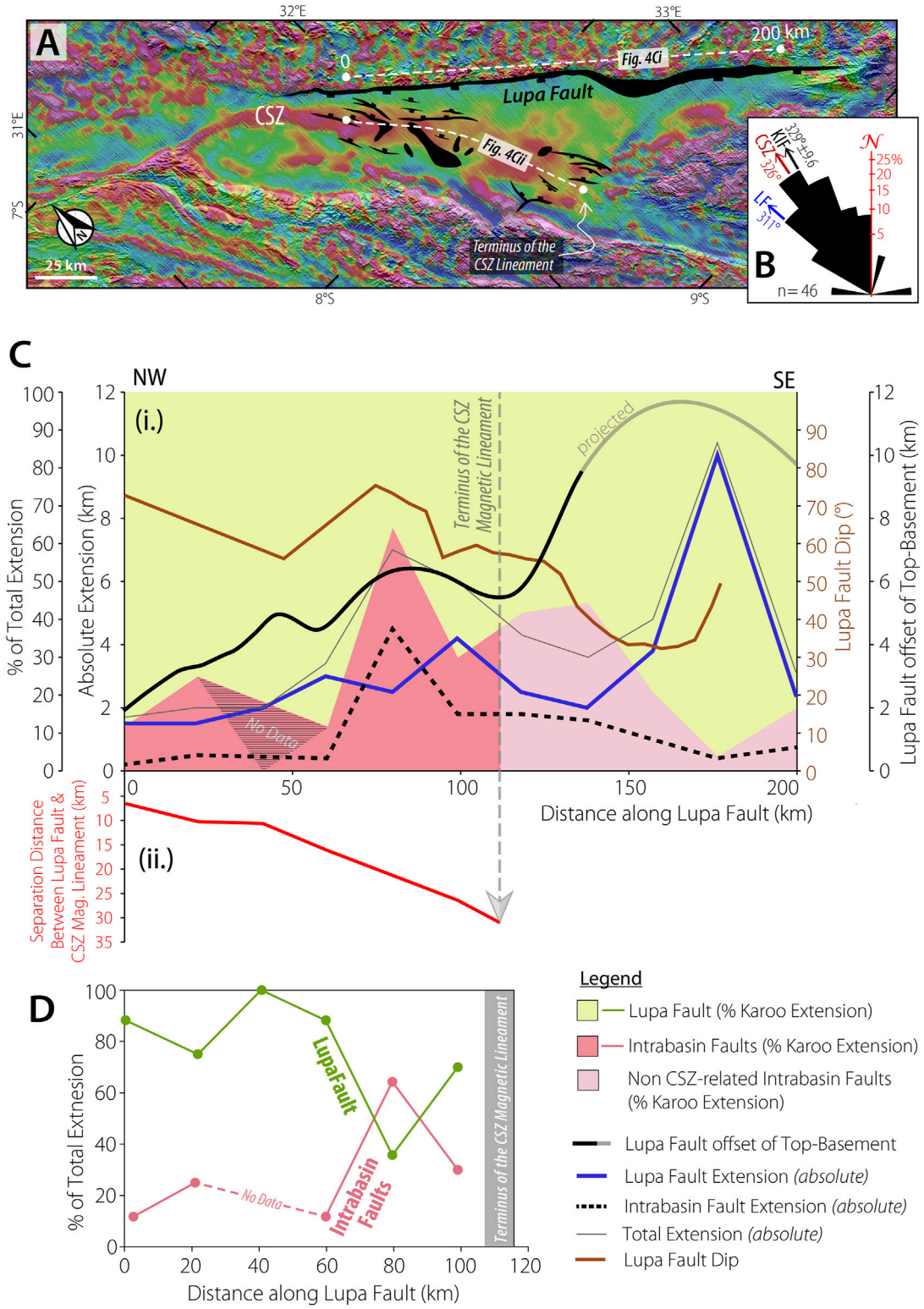

FIGURE 4 | (A): Map of vertical derivative of the aeromagnetic grid overlaid on satellite DEM hillshade map, showing the section of the Rukwa Rift (white dashed lines) along which, the measurements plotted in **Figures 4C,D** were taken. **(B)**: Frequency-azimuth distribution of the Karoo-age intra-basinal faults (KIF; measured in this study). CSZ = Chisi Shear Zone, LF = Lupa Fault. Arrows represent the mean trend of the associated structure. **(C)**: Plot showing along-rift distribution of **(i.)** line-length measurement of the Top-Karoo surface as estimates of Karoo-age tectonic extension (for the Lupa and intra-basinal faults), Lupa Fault dip angle, and Top-Basement offset along the Lupa Fault, and **(ii.)** lateral separation distance between the CSZ and the Lupa Fault. **(D)**: Plot showing the along-rift variation of % total Karoo-age extension accommodated by the Lupa Fault and the intra-basinal faults up till the CSZ termination (displayed as stacked area plot in **Figure 4C**).

Ubwari Ridge (buried horst and subaerial peninsula; **Figure 1B**, **Supplementary Figures S1A-B**). Although the Ubwari Ridge is a fault-bounded horst block in the Cenozoic Tanganyika Rift, its possible spatial association with the CSZ inferred based on both the colinearity with the continuation of the magnetic-high anomaly lineament of the CSZ, and the southeastward rotation of the N-trending metamorphic fabrics of the subaerial section of the horst (**Supplementary Figures S1B**, **S2B**).

The CSZ extends southeastwards from the Chisi area to continue beneath the Rukwa Rift, where it is sub-parallel to the rift border faults (**Figure 1B**, **2A**). Just southeast of the termination of the CSZ magnetic lineament, the >15 km-wide Mughese Shear Zone (MSZ) which separates the Ufipa and Mbozi Terranes of the Ubendian Belt (**Figure 1B**), extends beneath the Msongano Trough (bifurcation of the Rukwa Rift) and continues southeast into the Karonga Basin (**Figure 1B**, **2B**). Overall, the CSZ-associated aeromagnetic and geomorphic structures extend for >600 km from the Luama and Tanganyika rifts, southeastwards through the Rukwa Rift (**Figure 1B**). Although our mapping suggests an along-trend and perhaps genetic relationship between the CSZ and the Mughese Shear Zone (**Figure 1B**), we clarify that at the time of this contribution, there is no available data demonstrating that the Mughese Shear Zone is also a subduction-related suture. In the absence of this information, we define the southeast termination of the CSZ as the termination zone of its magnetic anomaly lineament beneath the Rukwa Rift (**Figure 1B**, **3A**).

Our 3D grid of the depth-distribution of intra-basement magnetic sources along the Rukwa Rift (**Figures 3A–C**, **Supplementary Figures S3A–B**, **S4A–B**) reveal a steeply-dipping, NW-trending zone of magnetic sources that extend to 12 km depth; this feature is spatially collocated with the surface trend of the CSZ aeromagnetic lineament (**Figure 3B**). Northeast of these CSZ-related magnetic sources, a narrow sub-vertical block of very shallow (<6 km deep) magnetic sources is spatially colocated with the Lupa Fault. This zone of Lupa Fault-related shallow sources separates the CSZ-related sources from another sub-vertical cluster of moderately deeper (~9 km-deep) magnetic sources that are spatially collocated with the Katuma Terrane (**Figures 3B–D**).

The CSZ and the Early-Rift (Karoo) Structure

The Karoo-age basin of the Rukwa Rift widens southeastwards from c. 16 km in the northwest to c. 57 km at the terminus of the CSZ magnetic lineament, before narrowing to <16 km towards the southeast (**Figure 2B**). The Karoo intra-basinal faults (KIF, 329° ± 9.6; **Figure 2Bi**) are dominated by a fault cluster, spaced 4–6 km apart and striking oblique to the Lupa Fault (311°). The fault cluster is collocated with the CSZ magnetic lineament and trends parallel to the lineament (**Figures 4A,B**). Although, some of the KIF faults dip to the SW, most of them dip to the NE (**Figure 2B**). A Karoo isopach map shows that the thickest sections (>1 km-thick) of the Karoo-age units are generally confined to the northeast of the CSZ anomaly (yellow polygon in **Figure 2B**; also see **Figures 2C,D**). Adjacent to the Katuma Terrane and CSZ lineament (i.e., northwestern half of the rift), the Lupa Fault has a relatively high dip (~69°); this decreases south-eastwards to <40° (**Figure 4C**). Also, within the rift, prominent basement ridges cluster along the CSZ, some of which appear to be fault-bounded (**Figure 2B**). We note the strong alignment between the CSZ mean trend (326°), KIF mean trend (329° ± 9.6), and that of all (Permian to Quaternary) rift faults (ARF, 330°; **Figure 2Bii**).

Strain Distribution Within the Rukwa Rift During Karoo Extension

In the northwestern half of the Rukwa Rift, the proportion of Karoo-phase tectonic extension accommodated by the KIF increased southeastwards from ~12 to 64% (**Figures 4C,D**). This trend is coincident with an increase in across-strike separation between the Lupa border fault and the CSZ, from <10 km in the NW to ~30 km at the SE terminus of CSZ magnetic lineament (**Figure 4C**; see also **Figure 4A**). However, southeastward from the CSZ terminus to the southeast tip of the basin, total extension was largely accommodated by the Lupa Fault (up to 83%; **Figure 4C**). Also, NW of the CSZ terminus, the curve for intra-basinal fault absolute extension tracks that of the total absolute extension, whereas SE of the CSZ terminus, total absolute extension curve is not tracked by that of the intra-basinal fault, rather, it is tracked by the Lupa Fault absolute extension (**Figure 4C**). The southeastward increase in the percentage of total extension accommodated by the Lupa Fault is consistent with the southeastward increase in the magnitude of Lupa Fault's offset of the Top-Basement which shows a more pronounced increase just southeast of the CSZ terminus (see "Lupa Fault offset of Top-Basement" curve in **Figure 4C**). Northwest of the CSZ terminus, Lupa Fault's offset of the Top-Basement shows a range of 2–6.4 km over a distance of 120 km, whereas SE of the CSZ terminus, the basement offset increases from ~5.5 km to >9 km within ~20 km distance.

CONTROLS OF THE CSZ AND TERRANE BOUNDARY ON EARLY-RIFT FAULTING, STRAIN DISTRIBUTION, AND BASIN ARCHITECTURE

Border Fault Development

The geometrical and spatial relationships between the Karoo rift-related structures, the CSZ, and the adjacent basement terrane boundaries reveal how strain was localized and spatially partitioned during the early phases of extension in the Rukwa Rift. The Lupa Fault is the largest rift-related structure in the Rukwa Rift, having formed at the very onset of rifting, thus representing the border fault (e.g., Kilembe and Rosendahl, 1992; Morley et al., 1992, 1999; Wheeler and Karson 1994). Studies suggest that the Lupa Fault localized along terrane boundaries (Katuma-Wakole boundary in the NW and Lupa-Mbozi boundary in the SE) and that its NW-SE trend is influenced by the structural fabrics in the bounding Katuma Terrane

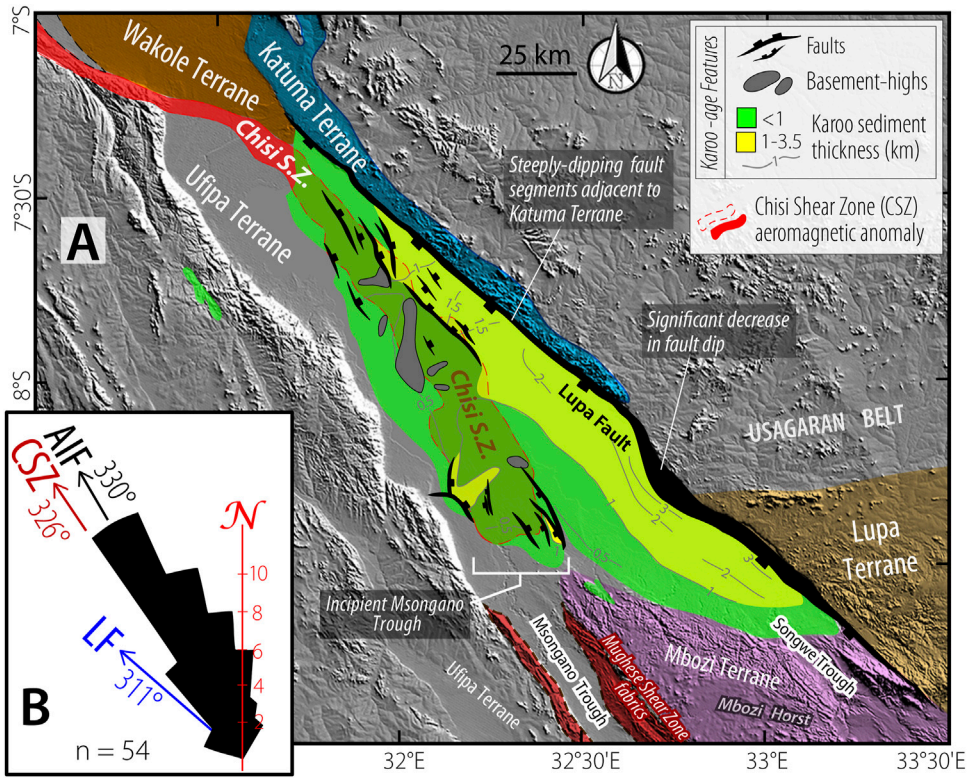

FIGURE 5 | (A): Satellite DEM hillshade map of the Rukwa Rift, overlaid with the Karoo structural features (faults and basement ridges), Karoo isopach map (from Morley et al., 1992, 1999), Chisi Shear Zone magnetic anomaly, and the relevant surrounding basement terranes. **(B)**: Frequency-azimuth distribution of all the faults (Permian-Quaternary) in the Rukwa Rift (digitized from Morley et al., 1992). ARF = "All Rukwa Rift faults" and black arrow showing their mean trend; LF = "Lupa Fault" and blue arrow showing its approximate trend; CSZ = "Chisi Shear Zone" and brown arrow showing its approximate trend within the rift axis.

(**Figures 1B**, **3B–D**; Daly et al., 1989; Wheeler and Karson, 1994; Theunissen et al., 1996; Lemna et al., 2019; Heilman et al., 2019). However, the observations supporting these hypotheses were based on the shallow geometries of structures observed in the field or the plan-view structural trends of metamorphic fabrics expressed in aeromagnetic data.

The sub-vertical dips described by the cluster of magnetic sources beneath the Katuma Terrane (**Figure 3B**) support previous studies that argue that the Katuma-Wakole terrane boundary, and fabrics within the Katuma Terrane, are steeply dipping. However, the Lupa Fault itself shows an abrupt and significant decrease in dip just southeast of the Katuma Terrane termination (**Figure 4C**), where it is coincident with the E-W-trending Usagaran Belt and Lupa Terrane (**Figure 5A**). Therefore, we suggest that both the Katuma-Wakole Terrane boundary and the tectonic structures in the Katuma Terrane are responsible for the steep dip of the Lupa border fault in the NW; in contrast, to the SE, the absence of favorably oriented intra-basement structures result in the fault having a lower dip.

The sub-vertical dip of the CSZ-related magnetic sources and southwest dip direction of the Lupa Fault (**Figure 3C**) also suggests that the deepest sections of the border fault could merge with the shear zone at the deeper crustal levels, although it would require a southwestward dip for the CSZ at depth. If this spatial and potentially kinematic relationship is true, we infer a depth-dependent partitioning of the control of structural inheritance on the early development of the Lupa border fault, such that the upper sections of the fault exploited the Katuma-Wakole Terrane boundary and structures in the Katuma Terrane, and the deepest section exploited the Chisi Shear Zone.

Intra-Basinal Faulting

The collocation and parallel trends of the KIF and CSZ suggest that the CSZ largely controlled the localization of the Karoo intra-basinal faulting (**Figure 4A**, **5A**). The prominence of NE-dip direction of the KIF faults (**Figure 4A**) suggests that the KIF exploited the NE-dipping metamorphic fabrics along the CSZ (**Figure 2A**). The confinement of the main Karoo-age rift fill between the Lupa Fault and CSZ (where present) (**Figure 5A**) indicates that the KIF cluster directly influenced the first-order sediment distribution during the early phases of extension. The Karoo-age basin is widest in the northwest where the CSZ is present (CSZ rotates from NW to NNW trend, away from the Lupa Fault), further indicating the influence of the CSZ and its geometry on the extent of the early rift-related depocenter (**Figure 4A**). The apparent confinement of earliest rift-related sediments also provides further age constraints on the timing of formation of the intra-basinal fault cluster. Overall, these observations indicate that the shear zone and terrane

boundary represent discrete zones of inherited mechanical weakness in the crust where brittle deformation was accommodated during the early stages of continental extension.

Early-Rift Paleotopography

The Karoo-age rift topography is likely dominated by the footwall uplift along the Lupa border fault in the northeastern basin margin (Van der Beek et al., 1998; Morley et al., 1999). However, the clustering of basement ridges along the submarine part of the CSZ, likely representative of early syn-rift erosionally-resistant topography, is consistent with observations of topographic ridges along the CSZ onshore (**Figure 1B** and **Supplementary Figure S2A**). Elsewhere, prominent, erosionally-resistant topographic ridges define the surface expression of the Mughese Shear Zone (Kolawole et al., 2018), which appears to be a southeast continuation of the CSZ trend in the Karonga Basin (**Figure 1B**). Such ridges represent elevated topographic domains that may represent important sediment sources (e.g., Gawthorpe and Leeder, 2000). Thus, the chain of ridges along the CSZ represents intra-basinal sediment-source regions near the southwestern basin margin, indicating an additional importance of the CSZ during initial sedimentation in the Rukwa Rift.

Early-Rift Distribution of Extension

Our analyses show that within the northwestern section of the basin, Karoo-age tectonic extension was largely accommodated on both the CSZ-related intra-basinal faults (KIF) and the Lupa border fault (**Figures 4C,D**); in fact, during this initial phase of extension, more strain was accommodated on intra-basinal faults than the (developing) border fault. In contrast, southeast of the CSZ termination beneath the basin (or at significantly large separation distance), extension was primarily accommodated along the Lupa border fault. These suggest that during the early phase of rifting, there was a competition for extensional strain localization between the CSZ and the Katuma-Wakole terrane boundary in the northwest. Due to the southward increase in separation between the CSZ and Katuma-Wakole/Lupa-Mbozi terrane boundaries, and the absence of CSZ in the southeastern section of the Karoo-age basin, tectonic extension was then primarily accommodated along the Lupa Fault, which ultimately exploited the Lupa-Mbozi terrane boundary (**Figures 4C,D**). The significant increase in the Lupa Fault Top-basement offset just south of the CSZ termination (**Figure 4C**) also supports the dominant localization of extensional strain on the border fault in the southeastern section of the basin where the CSZ-related KIF is absent. Thus, we suggest that the CSZ strongly controlled the early-phase distribution of tectonic extension along the Rukwa Rift.

This along-rift partitioning of strain resulted in a lateral change of the overall Karoo-age rift geometry from a shallower graben in the northwest, to a deep half graben in the southeast. This along-rift change in rift geometry was previously thought to be primarily related to variation in border fault strain accommodation controlled by oblique extensional kinematics (Morley et al., 1992). Also, the obliquity of the intra-basinal faults relative to the border fault trend (**Figures 4B**, **5B**) has been used as a basis for inferring pull-apart and oblique extension kinematics for the rift development (Kilembe and Rosendahl, 1992; Chattopadhyay and Chakra, 2013). However, detailed structural interpretation from seismic reflection data revealed a minor component of strike-slip-related deformation along the rift (Morley et al., 1999). Thus, we here suggest that the observed obliquity of intra-basinal faults to border fault trend is primarily controlled by the focusing of extensional strain along prominent pre-existing discrete zones of basement weakness during the early phase of rifting. The geometrical alignment of the intra-basinal faults to the CSZ trend could have been influenced by local stress rotation (SHmax) into CSZ-parallel/sub-parallel trend during the early rift phase; a mechanism that has been proposed to explain the influence of weak basement fabrics on the present-day orthogonal extension kinematics along the Rukwa Rift (Morley, 2010). This resolves a long-standing controversy related to the geometrical structure and kinematics of rift faulting in the Rukwa Rift. Elsewhere along the Rukwa Trend, farther northwest of the Rukwa Rift, the Busindi border fault of the Luama Rift exploited the NW continuation of the CSZ (**Figures 1B**, **3D**), demonstrating the broader influence of the CSZ on the development of the other Karoo rift segments of the Rukwa Trend. In the Tanganyika Rift, the along-rift distribution of tectonic extension is influenced by the lateral variation of the inherited crustal rheology (Wright et al., 2020), further demonstrating the strong influence of structural inheritance on the early localization and distribution of extension along continental rifts.

Post-Karoo Rift Architecture

Geological and geophysical evidence for post-Karoo strike-slip deformation has been recorded along the Rukwa Rift (Wheeler and Karson, 1994; Delvaux et al., 2012; Heilman et al., 2019), possibly associated with a plate-scale compressional event (Daly et al., 1991; Delvaux et al., 2021). However, the analyses of seismic reflection profiles across the Rukwa Rift show that post-Karoo strike-slip or compressional deformation in the basin was very minor (Morley et al., 1999). Therefore, it is not likely that the plate-scale compressional event significantly altered the karoo-age fault patterns in the Rukwa Rift.

The CSZ and adjacent terrane boundaries continued and still continue to influence rift geometry long after the Karoo phase of extension. First, the mean trend of the rift faults, all combined (Permian to Quaternary), generally remains the same as the Karoo-age mean intra-basinal fault trend (**Figures 2Bi–ii**; Morley et al., 1992; Kilembe and Rosendahl, 1992). Second, the along-strike projection of the CSZ southeast of its magnetic anomaly termination is coincident with location and orientation of the Msongano Trough, which represents a southeastward continuation of the Rukwa Rift during the Cenozoic rifting phase (**Figure 5A**). We suggest that the extension of the KIF to the CSZ termination zone already established the incipient graben of the Msongano Trough during the Karoo rifting phase (**Figure 5A**, **6**). We suggest that the CSZ and its colinear Mughese Shear Zone, along which the Msongano Trough developed (**Figure 5A**), both constitute coupled discrete zones of weakness in the basement that accommodated the continuous lateral southeastward propagation of the KIF as a narrow graben during the post-Karoo phases of extension. Thus, the present-day bifurcation of the Rukwa Rift into the Songwe and Msongano troughs

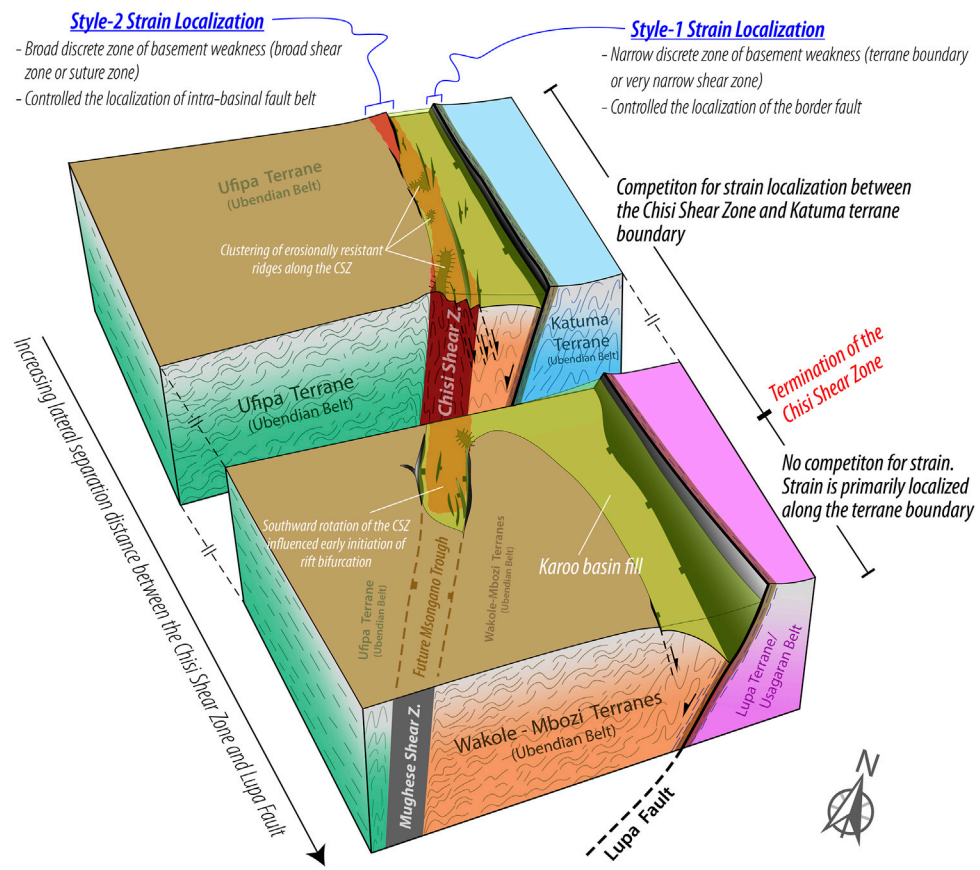

FIGURE 6 | Cartoon illustrating some of the key observations in this study, showing how the structure of discrete zones of basement weakness influenced strain localization styles and along-rift distribution of extension during the early phase of tectonic extension in the Rukwa Rift.

(**Figure 1C**) was established during the very earliest stage of rifting. In addition, the southeastern border fault of the Rukwa Rift (Ufipa Fault; **Figure 2B**) which developed in the Cenozoic, largely exploited the tectonic fabrics of the Ufipa Terrane (Heilman et al., 2019).

More broadly, in the Cenozoic Tanganyika Rift, located northwest of the Rukwa Rift (**Figures 1A,B**), the rift basin is segmented (Sander and Rosendahl, 1989; Muirhead et al., 2019; Wright et al., 2020). The segmentation occurs at the proposed splay of the CSZ magnetic lineaments (**Figure 1B**). The Ruzizi and East Kigoma sub-basins are separated by the northern section of the East CSZ splay, whereas the East and West Kigoma sub-basins are separated by the southern section of the East Splay, and the West Kigoma and Kalemie Sub-basins are separated by the CSZ segment extending into the Luama Rift. In essence, not only did the CSZ influence the early-phase architecture of the Karoo-age Rukwa and Luama rift basins, but also the structure of the relatively younger Tanganyika Rift. The spatial collocation of Cenozoic hydrothermal vents within different sections of the CSZ in the Tanganyika Rift (diamond symbols in **Figure 1B**) highlights the deep reaches of the rift faults that exploited the basement weakness of the shear zone.

Implications for Early-Stage Architecture of Continental Rift Basins

Our study of the Rukwa Rift suggests that early-phase rift strain is significantly accommodated by intra-basinal faults, contrary to observations in some other juvenile magma-poor continental rifts (e.g., Nixon et al., 2016; Muirhead et al., 2019), but it is localized onto pre-existing structures. The early-phase strain localization in the Rukwa Rift occurred via two different styles with associated deformational mechanisms. One style (Style-1 strain localization) is the localization of a large rift fault onto a narrow discrete zone of basement weakness, such as prominent basement terrane boundaries (this study), pre-existing fault zones, and narrow ductile shear zones, in which case the structures of the weak zone and the fabrics of the adjacent basement may influence the fault geometry (**Figure 6**). An example of this is the development of the Livingstone Fault in the Karonga Basin, northern Malawi Rift (Wheeler and Karson, 1989), the Thyolo border fault in the Shire Rift Zone (Wedmore et al., 2020b), and splay faulting at a terrane boundary during the Late Cretaceous extension between Zealandia and Australia (Phillips and McCaffrey, 2019b). A second style (Style-2 strain localization) is the localization of a fault cluster (or fault belt) onto a broader discrete zone of

basement weakness, such as wide pre-rift shear zones or subduction suture zones (this study), in which case the individual fault strands may exploit the smaller-scale mechanical heterogeneities within the broad zone of basement weakness (**Figure 6**). An example of Style-2 localization is the development of a fault cluster along the western margin of the Karonga Basin, northern Malawi Rift, where the fault cluster exploited the >15 km-wide Precambrian Mughese Shear Zone (Kolawole et al., 2018). Therefore, we hypothesize that during the earliest stages of continental rifting, strain initially localizes on pre-existing zones of crustal weakness, and the style of localization may be associated with the type of the inheritance and character of the inherited structure. In addition, we note that whilst pre-existing structure may exert a strong control on strain distribution and localization during the earliest phase of continental extension, the established early rift template, may persist through the subsequent phases of the stretching stage of rifting (i.e., prior to the necking and hyper-extension stages).

CONCLUSION

We investigated the distribution of strain during the earliest phase of extension in the Rukwa Rift, a Phanerozoic multiphase magma-poor rift basin that developed along the trend of the Precambrian Chisi Shear Zone (CSZ) and terrane boundary shear zones in East Africa.

Here are our main findings:

1) During the earliest phase of extension, although the border fault, Lupa Fault exploited the colinear Katuma-Wakole and Lupa-Mbozi terrane boundaries, the CSZ facilitated the early localization and development of a prominent intra-basinal fault cluster.
2) In the northwestern section of the rift, the presence and proximity of the CSZ and the Katuma-Wakole terrane boundary facilitated a competition for strain localization between the CSZ and the adjacent terrane boundary, whereas in the southeastern section where the CSZ is either absent or at a significantly large distance, strain is primarily localized along the Lupa-Mbozi terrane boundary.
3) The along-rift variation in early phase rift geometry, rift margin paleotopography, and depocenter extents were largely controlled by the CSZ.
4) The along-rift distribution of early-phase extension was largely influenced by structural inheritance, such that in the northwestern section of the rift, significant extension is accommodated by the intra-basinal fault cluster that exploited the CSZ, whereas in the southeast, extension is largely accommodated by the Lupa border fault.
5) Two styles of early-phase strain localization in which a.) strain is localized onto a narrow discrete zone of basement weakness in the form of a large rift fault (Style-1 strain localization), and b.) strain is localized onto a broad discrete zone of basement weakness in the form of a fault cluster (Style-2 strain localization).
6) Whilst pre-existing basement structure may exert the strong control on strain distribution and localization during the earliest phase of extension, the established early rift template, may persist through the subsequent phases of the stretching stage of rifting.

Our findings offer a window into the early stages of continental extension along a young evolving magma-poor rift, where early strain is not accommodated only by the border fault as suggested by existing magma-poor early-rift models; instead, strain focuses relatively quickly on a large border fault and intra-basinal fault clusters that follow pre-existing intra-basement structures. This study reveals the influence of structural inheritance on early-phase rift geometry and along-rift partitioning of strain along magma-poor rift basins.

DATA AVAILABILITY STATEMENT

Publicly available datasets were analyzed in this study. This data can be found here: The SADC aeromagnetic data is archived at http://sadc-gla.org/SADC/home.html. We have provided uninterpreted versions of the aeromagnetic data in our **Supplementary Material** document. The 2-D seismic reflection images of the Rukwa Rift shown in this study other 2-D seismic datasets from the basin are archived in the appendix of Morley et al. (1999), AAPG).

AUTHOR CONTRIBUTIONS

FK conceptualized and developed the project. FK and TP conducted the analyses and investigations. FK wrote the manuscript. TP, CJ, and EA edited and improved the manuscript. All authors read and approved the final manuscript.

ACKNOWLEDGMENTS

We thank reviewers Giacomo Corti and Damien Delvaux for their insightful comments that have helped to improve the quality of our paper, and we also thank the editor, James Muirhead for handling our paper. We thank Obeid Lemna for providing useful comments on the preprint of the initial version of the manuscript uploaded on EarthArXiv. We thank the South African Council for Geoscience for providing the aeromagnetic data to EA used in this study. The aeromagnetic data is archived at http://sadc-gla.org/SADC/home.html. We have provided uninterpreted versions of the aeromagnetic data in our **Supplementary Material** document. The seismic reflection cross-section of the Rukwa Rift shown in this study (**Figure 2C**) and other 2-D seismic datasets from the basin are archived in the appendix of Morley et al. (1999).

SUPPLEMENTARY MATERIAL

The Supplementary Material for this article can be found online at: https://www.frontiersin.org/articles/10.3389/feart.2021.707869/full#supplementary-material

REFERENCES

Agostini, A., Bonini, M., Corti, G., Sani, F., and Mazzarini, F. (2011). Fault Architecture in the Main Ethiopian Rift and Comparison with Experimental Models: Implications for Rift Evolution and Nubia–Somalia Kinematics. *Earth Planet. Sci. Lett.* 301 (3-4), 479–492. doi:10.1016/j.epsl.2010.11.024

Baranov, V. (1957). A New Method for Interpretation of Aeromagnetic Maps: Pseudo-gravimetric Anomalies. *Geophysics* 22 (2), 359–382. doi:10.1190/1.1438369

Boniface, N., Schenk, V., and Appel, P. (2012). Paleoproterozoic Eclogites of MORB-type Chemistry and Three Proterozoic Orogenic Cycles in the Ubendian Belt (Tanzania): Evidence from Monazite and Zircon Geochronology, and Geochemistry. *Precambrian Res.* 192-195, 16–33. doi:10.1016/j.precamres.2011.10.007

Boniface, N., and Schenk, V. (2012). Neoproterozoic Eclogites in the Paleoproterozoic Ubendian belt of Tanzania: Evidence for a Pan-African Suture between the Bangweulu Block and the Tanzania Craton. *Precambrian Res.* 208-211, 72–89. doi:10.1016/j.precamres.2012.03.014

Boven, A., Theunissen, K., Sklyarov, E., Klerkx, J., Melnikov, A., Mruma, A., et al. (1999). Timing of Exhumation of a High-Pressure Mafic Granulite Terrane of the Paleoproterozoic Ubende belt (West Tanzania). *Precambrian Res.* 93 (1), 119–137. doi:10.1016/s0301-9268(98)00101-6

Buiter, S. J. H., and Torsvik, T. H. (2014). A Review of Wilson Cycle Plate Margins: a Role for Mantle Plumes in continental Break-Up along Sutures? *Gondwana Res.* 26, 627–653. doi:10.1016/j.gr.2014.02.007

Chattopadhyay, A., and Chakra, M. (2013). Influence of Pre-existing Pervasive Fabrics on Fault Patterns during Orthogonal and Oblique Rifting: an Experimental Approach. *Mar. Pet. Geology.* 39 (1), 74–91. doi:10.1016/j.marpetgeo.2012.09.009

Chorowicz, J. (2005). The East African Rift System. *J. Afr. Earth Sci.* 43 (1-3), 379–410. doi:10.1016/j.jafrearsci.2005.07.019

Cowie, P. A., Underhill, J. R., Behn, M. D., Lin, J., and Gill, C. E. (2005). Spatio-Temporal Evolution of Strain Accumulation Derived from Multi-Scale Observations of Late Jurassic Rifting in the Northern North Sea: A Critical Test of Models for Lithospheric Extension. *Earth Planet. Sci. Lett.* 234 (3-4), 401–419.

Daly, M. C., Chorowicz, J., and Fairhead, J. D. (1989). Rift basin Evolution in Africa: The Influence of Reactivated Steep Basement Shear Zones. *Geol. Soc. Lond. Spec. Publications* 44 (1), 309–334. doi:10.1144/gsl.sp.1989.044.01.17

Daly, M. C. (1988). Crustal Shear Zones in Central Africa: a Kinematic Approach to Proterozoic Tectonics. *Episodes* 11 (1), 5–11. doi:10.18814/epiiugs/1988/v11i1/003

Daly, M. C., Lawrence, S. R., Kimun'a, D., and Binga, M. (1991). Late Palaeozoic Deformation in central Africa: a Result of Distant Collision? *Nature* 350 (6319), 605–607. doi:10.1038/350605a0

Delvaux, D. (2001). *Karoo Rifting in Western Tanzania: Precursor of Gondwana Breakup. Contributions to Geology and Paleontology of Gondwana in Honor of Helmut Wopfner*:. Cologne: Geological Institute, University of Cologne, 111–125.

Delvaux, D., Kervyn, F., Macheyeki, A. S., and Temu, E. B. (2012). Geodynamic Significance of the TRM Segment in the East African Rift (W-Tanzania): Active Tectonics and Paleostress in the Ufipa Plateau and Rukwa basin. *J. Struct. Geology.* 37, 161–180. doi:10.1016/j.jsg.2012.01.008

Delvaux, D., Maddaloni, F., Tesauro, M., and Braitenberg, C. (2021). The Congo Basin: Stratigraphy and Subsurface Structure Defined by Regional Seismic Reflection, Refraction and Well Data. *Glob. Planet. Change* 198, 103407. doi:10.1016/j.gloplacha.2020.103407

Dewey, J., and Spall, H. (1975). Pre-Mesozoic Plate Tectonics: How Far Back in Earth History Can the Wilson Cycle Be Extended? *Geol* 3, 422–424. doi:10.1130/0091-7613(1975)3<422:ppthfb>2.0.co;2

Ebinger, C. (2005). Continental Break-Up: the East African Perspective. *Astron. Geophys.* 46 (2), 2–16. doi:10.1111/j.1468-4004.2005.46216.x

Ganbat, A., Tsujimori, T., Boniface, N., Pastor-Galán, D., Aoki, S., and Aoki, K. (2021). Crustal Evolution of the Paleoproterozoic Ubendian Belt (SW Tanzania) Western Margin: A Central African Shield Amalgamation Tale. *Gondwana Res.* 91, 286–306. doi:10.1016/j.gr.2020.12.009

Gawthorpe, R. L., and Leeder, M. R. (2008). Tectono-sedimentary Evolution of Active Extensional Basins. *Basin Res.* 12 (3-4), 195–218. doi:10.1111/j.1365-2117.2000.00121.x

Hayward, N. J., and Ebinger, C. J. (1996). Variations in the along-axis Segmentation of the Afar Rift System. *Tectonics* 15 (2), 244–257. doi:10.1029/95tc02292

Heilman, E., Kolawole, F., Atekwana, E. A., and Mayle, M. (2019). Controls of Basement Fabric on the Linkage of Rift Segments. *Tectonics* 38 (4), 1337–1366. doi:10.1029/2018tc005362

Hodgson, I., Illsley-Kemp, F., Gallacher, R. J., Keir, D., Ebinger, C. J., and Mtelela, K. (2017). Crustal Structure at a Young continental Rift: A Receiver Function Study from the Tanganyika Rift. *Tectonics* 36 (12), 2806–2822. doi:10.1002/2017tc004477

Kilembe, E. A., and Rosendahl, B. R. (1992). "Structure and Stratigraphy of the Rukwa Rift," in *Tectonophysics*. Editors C. J. Ebinger, H. K. Gupta, and L.O. Nyambok (Nairobi, Kenya: Seismology and Related Sciences in Africa), 209, 143–158. doi:10.1016/0040-1951(92)90016-y

Klerkx, J., Theunissen, K., and Delvaux, D. (1998). Persistent Fault Controlled basin Formation since the Proterozoic along the Western Branch of the East African Rift. *J. Afr. Earth Sci.* 26 (3), 347–361. doi:10.1016/s0899-5362(98)00020-7

Kolawole, F., Atekwana, E. A., Laó-Dávila, D. A., Abdelsalam, M. G., Chindandali, P. R., Salima, J., et al. (2018). Active Deformation of Malawi Rift's north basin Hinge Zone Modulated by Reactivation of Preexisting Precambrian Shear Zone Fabric. *Tectonics* 37 (3), 683–704. doi:10.1002/2017tc004628

Kolawole, F., Atekwana, E. A., Malloy, S., Stamps, D. S., Grandin, R., Abdelsalam, M. G., et al. (2017). Aeromagnetic, Gravity, and Differential Interferometric Synthetic Aperture Radar Analyses Reveal the Causative Fault of the 3 April 2017Mw6.5 Moiyabana, Botswana, Earthquake. *Geophys. Res. Lett.* 44 (17), 8837–8846. doi:10.1002/2017gl074620

Lemna, O. S., Stephenson, R., and Cornwell, D. G. (2019). The Role of Pre-existing Precambrian Structures in the Development of Rukwa Rift Basin, Southwest Tanzania. *J. Afr. Earth Sci.* 150, 607–625. doi:10.1016/j.jafrearsci.2018.09.015

Lenoir, J. L., Liégeois, J.-P., Theunissen, K., and Klerkx, J. (1994). The Palaeoproterozoic Ubendian Shear belt in Tanzania: Geochronology and Structure. *J. Afr. Earth Sci.* 19 (3), 169–184. doi:10.1016/0899-5362(94)90059-0

Morley, C. K., Cunningham, S. M., Harper, R. M., and Wescott, W. A. (1992). Geology and Geophysics of the Rukwa Rift, East Africa. *Tectonics* 11 (1), 69–81. doi:10.1029/91tc02102

Morley, C. K. (2010). Stress Re-orientation along Zones of Weak Fabrics in Rifts: An Explanation for Pure Extension in 'oblique' Rift Segments? *Earth Planet. Sci. Lett.* 297 (3-4), 667–673. doi:10.1016/j.epsl.2010.07.022

Morley, C. K., Wescott, W. A., Harper, R. M., and Cunningham, S. M. (1999). Geology and Geophysics of the Rukwa Rift. Geoscience of Rift Systems-Evolution of East Africa. *AAPG Stud. Geology.* 44, 91–110.

Muirhead, J. D., Kattenhorn, S. A., Lee, H., Mana, S., Turrin, B. D., Fischer, T. P., et al. (2016). Evolution of Upper Crustal Faulting Assisted by Magmatic Volatile Release during Early-Stage continental Rift Development in the East African Rift. *Geosphere* 12, 1670–1700. doi:10.1130/ges01375.1

Muirhead, J. D., Wright, L. J. M., and Scholz, C. A. (2019). Rift Evolution in Regions of Low Magma Input in East Africa. *Earth Planet. Sci. Lett.* 506, 332–346. doi:10.1016/j.epsl.2018.11.004

Naliboff, J. B., Buiter, S. J., Péron-Pinvidic, G., Osmundsen, P. T., and Tetreault, J. (2017). Complex Fault Interaction Controls continental Rifting. *Nat. Commun.* 8 (1), 1–9. doi:10.1038/s41467-017-00904-x

Nixon, C. W., McNeill, L. C., Bull, J. M., Bell, R. E., Gawthorpe, R. L., Henstock, T. J., et al. (2016). Rapid Spatiotemporal Variations in Rift Structure during Development of the Corinth Rift, central Greece. *Tectonics* 35 (5), 1225–1248. doi:10.1002/2015tc004026

Osagiede, E. E., Rotevatn, A., Gawthorpe, R., Kristensen, T. B., Jackson, C. A.-L., and Marsh, N. (2020). Pre-existing Intra-basement Shear Zones Influence Growth and Geometry of Non-colinear normal Faults, Western Utsira High-Heimdal Terrace, North Sea. *J. Struct. Geology.* 130, 103908. doi:10.1016/j.jsg.2019.103908

Phillips, T. B., Fazlikhani, H., Gawthorpe, R. L., Fossen, H., Jackson, C. A. L., Bell, R. E., et al. (2019a). The Influence of Structural Inheritance and Multiphase Extension on Rift Development, the Northern North Sea. *Tectonics* 38. doi:10.1029/2019tc005756

Phillips, T. B., and McCaffrey, K. J. W. (2019b). Terrane Boundary Reactivation, Barriers to Lateral Fault Propagation and Reactivated Fabrics: Rifting across the Median Batholith Zone, Great South Basin, New Zealand. *Tectonics* 38 (11), 4027–4053. doi:10.1029/2019tc005772

Ragon, T., Nutz, A., Schuster, M., Ghienne, J. F., Ruffet, G., and Rubino, J. L. (2019). Evolution of the Northern Turkana Depression (East African Rift System, Kenya) during the Cenozoic Rifting: New Insights from the Ekitale Basin (28-25.5 Ma). *Geol. J.* 54 (6), 3468–3488. doi:10.1002/gj.3339

Roberts, E. M., O'Connor, P. M., Stevens, N. J., Gottfried, M. D., Jinnah, Z. A., Ngasala, S., et al. (2010). Sedimentology and Depositional Environments of the Red Sandstone Group, Rukwa Rift Basin, Southwestern Tanzania: New Insight into Cretaceous and Paleogene Terrestrial Ecosystems and Tectonics in Sub-equatorial Africa. *J. Afr. Earth Sci.* 57 (3), 179–212. doi:10.1016/j.jafrearsci.2009.09.002

Roberts, E. M., Stevens, N. J., O'Connor, P. M., Dirks, P. H. G. M., Gottfried, M. D., Clyde, W. C., et al. (2012). Initiation of the Western branch of the East African Rift Coeval with the Eastern branch. *Nat. Geosci* 5 (4), 289–294. doi:10.1038/ngeo1432

Salem, A., Williams, S., Fairhead, J. D., Smith, R., and Ravat, D. (2007). Interpretation of Magnetic Data Using Tilt-Angle Derivatives. *Geophysics* 73 (1), L1–L10.

Schiffer, C., Doré, A. G., Foulger, G. R., Franke, D., Geoffroy, L., Gernigon, L., et al. (2019). Structural Inheritance in the North Atlantic. *Earth-Science Rev.*.

Sklyarov, E. V., Theunissen, K., Melnikov, A. I., Klerkx, J., Gladkochub, D. P., and Mruma, A. (1998). Paleoproterozoic Eclogites and Garnet Pyroxenites of the Ubende Belt (Tanzania). *Schweizerische Mineralogische Petrographische Mitteilungen* 78, 257–271.

Smirnov, V., Pentelkov, V., Tolochko, V., Trifan, M., and Zhukov, S. (1973). *Geology and Minerals of the central Part of the Western Rift. Tech. rep., Mineral and Resource Division, Dodoma, Tanzania*. Dodoma, Tanzania: Unpublished report of the geological mapping. doi:10.1007/978-1-4684-1968-9

Theunissen, K., Klerkx, J., Melnikov, A., and Mruma, A. (1996). Mechanisms of Inheritance of Rift Faulting in the Western branch of the East African Rift, Tanzania. *Tectonics* 15 (4), 776–790. doi:10.1029/95tc03685

Van der Beek, P., Mbede, E., Andriessen, P., and Delvaux, D. (1998). Denudation History of the Malawi and Rukwa Rift Flanks (East African Rift System) from Apatite Fission Track Thermochronology. *J. Afr. Earth Sci.* 26 (3), 363–385. doi:10.1016/s0899-5362(98)00021-9

Wang, L., Maestrelli, D., Corti, G., Zou, Y., and Shen, C. (2021). Normal Fault Reactivation during Multiphase Extension: Analogue Models and Application to the Turkana Depression, East Africa. *Tectonophysics* 811, 228870. doi:10.1016/j.tecto.2021.228870

Wedmore, L. N., Biggs, J., Williams, J. N., Fagereng, Å., Dulanya, Z., Mphepo, F., et al. (2020a). Active Fault Scarps in Southern Malawi and Their Implications for the Distribution of Strain in Incipient continental Rifts. *Tectonics* 39 (3), e2019TC005834. doi:10.1029/2019tc005834

Wedmore, L. N. J., Williams, J. N., Biggs, J., Fagereng, Å., Mphepo, F., Dulanya, Z., et al. (2020b). Structural Inheritance and Border Fault Reactivation during Active Early-Stage Rifting along the Thyolo Fault, Malawi. *J. Struct. Geology.* 139, 104097. doi:10.1016/j.jsg.2020.104097

Wheeler, W. H., and Karson, J. A. (1994). Extension and Subsidence Adjacent to a "weak" continental Transform: An Example from the Rukwa Rift, East Africa. *Geol* 22 (7), 625–628. doi:10.1130/0091-7613(1994)022<0625:easata>2.3.co;2

Wheeler, W. H., and Karson, J. A. (1989). Structure and Kinematics of the Livingstone Mountains Border Fault Zone, Nyasa (Malawi) Rift, Southwestern Tanzania. *J. Afr. Earth Sci. (and Middle East)* 8 (2-4), 393–413. doi:10.1016/s0899-5362(89)80034-x

Wilson, J. T. (1966). Did the Atlantic Close and Then Re-open? *Nature* 211, 676–681. doi:10.1038/211676a0

Wright, L. J. M., Muirhead, J. D., and Scholz, C. A. (2020). Spatiotemporal Variations in Upper Crustal Extension across the Different Basement Terranes of the Lake Tanganyika Rift, East Africa. *Tectonics* 39, e2019TC006019. doi:10.1029/2019tc006019

Conflict of Interest: FK is currently employed by BP America. However, this study and the initial manuscript drafts were developed and completed during his stay at the University of Oklahoma, prior to joining BP.

The remaining authors declare that the research was conducted in the absence of any commercial or financial relationships that could be construed as a potential conflict of interest.

Publisher's Note: All claims expressed in this article are solely those of the authors and do not necessarily represent those of their affiliated organizations, or those of the publisher, the editors and the reviewers. Any product that may be evaluated in this article, or claim that may be made by its manufacturer, is not guaranteed or endorsed by the publisher.

Copyright © 2021 Kolawole, Phillips, Atekwana and Jackson. This is an open-access article distributed under the terms of the Creative Commons Attribution License (CC BY). The use, distribution or reproduction in other forums is permitted, provided the original author(s) and the copyright owner(s) are credited and that the original publication in this journal is cited, in accordance with accepted academic practice. No use, distribution or reproduction is permitted which does not comply with these terms.